High-speed multi-beam X-ray imaging using a lens coupling detector system

著者	Tetsuroh Shirasawa, Liang Xiaouyu, Wolfgang Voegeli, Etsuo Arakawa, Kentaro Kajiwara, Wataru Yashiro
journal or publication title	Applied Physics Express
volume	13
number	7
page range	077002
year	2020-06-26
URL	http://hdl.handle.net/10097/00131991

doi: 10.35848/1882-0786/ab9d30

High-speed multi-beam X-ray imaging using a lens coupling detector system

Tetsuroh Shirasawa[1], Liang Xiaouyu[2], Wolfgang Voegeli[3], Etsuo Arakawa[3], Kentaro Kajiwara[4], and Wataru Yashiro[2]*

[1]*National metrology Institute of Japan (NMIJ), National Institute of Advanced Industrial Science and Technology (AIST), Tsukuba, Ibaraki 305-8565, Japan*

[2]*Institute of Multidisciplinary Research for Advanced Materials (IMRAM), Tohoku University, Katahira, Sendai 980-8577, Japan*

[3]*Department of Physics, Tokyo Gakugei University, Koganei, Tokyo 184-8501, Japan*

[4]*Japan Synchrotron Radiation Research Institute (JASRI), Sayo, Hyogo 679-5198, Japan*

*E-mail: wyashiro@tohoku.ac.jp

Abstract

We present a high-speed multi-beam X-ray imaging realized using a detector system and the recently developed multi-beam X-ray optics [Voegeli et al., Optica **7**, 514 (2020)]. The detector utilized optical relay lenses and mirrors for connecting four scintillator screens to a CMOS camera, enabling the high-speed simultaneous acquisition of multiple projection images. We successfully acquired nine projection images in 0.5 ms with a spatial resolution of 70 μm. Dynamical behaviors of a light-bulb filament and a living ladybug were captured with a temporal resolution of 0.5 ms, demonstrating the potential for high-speed and high-spatial-resolution 4D X-ray tomography.

With growing interest in dynamical phenomena in various fields of fundamental and industrial sciences, demand for accessing internal structures of objects with high spatial and temporal resolutions has been increasing. X-ray imaging is often used to visualize internal microstructures of a wide variety of objects non-destructively, which even include weakly X-ray-absorbing objects by virtue of phase-contrast imaging techniques.[1-24)] The high-speed X-ray imaging has been developed significantly in the past two decades, largely due to the availability of high-brilliance synchrotron radiation (SR) sources and X-ray free-electron lasers. These X-ray sources realized the high-spatial-resolution (on the order of or better than 10 μm) two-dimensional (2D) imaging with a temporal resolution even better than μs.[25-34)]

For the 3D imaging of non-repeatable phenomena, generally the temporal resolution becomes worse since the depth-resolved visualization requires a rotation of the sample. In particular, a 3D tomographic reconstruction requires a few hundred projection images, and eventually the temporal resolution would be as low as subsecond.[35-38)] A conceptually simple approach to the faster data acquisition is to increase the speed of sample rotation. By using this approach, 4D tomography with a temporal resolution of a few ms and a spatial resolution of a few tens of μm was realized,[21,28,29,34)] and an even higher temporal resolution can be achieved by applying data processing techniques such as compressed sensing and interior tomography to a smaller number of projection data.[29,39-42)] However, such a high-speed rotation is incompatible with a sample that is affected by the centrifugal force arising from the rotation, e.g., living beings and fluids.

X-ray multi-beam technique,[43-45)] which can illuminate a sample from multiple directions simultaneously, is an alternative promising approach to the high-speed 4D tomography. Hoshino *et al*. developed three-beam imaging system using a direct SR beam and two Bragg-reflected beams from Si single crystals, and succeeded in capturing motions of heart and lungs of a living mouse with a temporal resolution of a few tens of ms.[43)] Villanueva-Perez *et al*. obtained three projection images simultaneously by using a Si single crystal and showed its potential extension to the nine-beam imaging.[44)] Recently, we have developed a multi-beam X-ray optics consisting of Si single-crystalline blades which can illuminate a sample from more than 30 different directions. Thirty-two projection images covering an angular range of more than ±70° were obtained without moving the sample and optics, and a 3D tomogram was successfully reconstructed with the help of a compressed sensing algorism.[45)] To realize the high-speed 4D tomography, a detector system is required that can simultaneously capture the multiple projection images, distributed in such a wide angular range, with high spatial and temporal resolutions.

Recently, we developed a detector system with a flexible branched optical fiber bundle, which was capable of simultaneous recording of four projection images on a single CMOS camera.[46] The system realized a spatially flexible detection of the multiple beams, however, the resulting spatial resolution was as low as 200 μm. In the present report, we show a detector system which realized the multi-beam X-ray imaging with a higher spatial resolution. We succeeded in the simultaneous detection of nine projection images of a sample in 0.5 ms with a spatial resolution of 70 μm. Non-repeatable dynamical phenomena were captured with a temporal resolution of 0.5 ms, suggesting its promising capability for the high-speed 4D tomography.

The layout of the multi-beam X-ray imaging is schematically illustrated in Fig. 1. The layout is similar to the previous study[46] except for the detector system. The experiment was performed at BL28B2 in SPring-8, Japan, and a white SR beam from a bending magnet was used. We used a component of the multi-beam X-ray optics[45], which consists of eight Si(001) single-crystalline blades aligned on a hyperbolic plane. Each of the blades diffracted X-rays by the (110) lattice planes and illuminated the sample, placed at the focus of the hyperbola, from a different angle. The X-ray beams passing through the sample was incident on the scintillator screens [Mitsubishi Chemical Corporation, DRZ-HR (Gd_2O_2S: Tb, thickness: 50 μm)], and the fluorescence were transferred through the relay lenses (magnification of 1) and mirrors to a CMOS camera (Photron FASTCAM Mini AX50, pixel size: 20 μm × 20 μm). The simultaneous acquisition using a single CMOS camera in a relatively small space (see the photo of Fig. 1) can solve the practical issues of cost and space for realizing the multi-beam X-ray imaging.

A part of the white SR beam directly impinging on the sample was also used to obtain a projection image. The image was recorded with a high-spatial-resolution detector consisting of a scintillator screen (Ce: $Gd_3Al_2Ga_3O_{12}$, thickness: 10 μm), a mirror, relay lenses, and a CMOS camera (Photron FASTCAM Nova S12 type 1000 K, effective pixel size: 4.6 μm × 4.6 μm). The transmittance of the projection image was calculated by $(I\text{-}B)/(I_0\text{-}B)$, where I and I_0 are the intensities with and without the sample, respectively, and B is the readout noise of a CMOS camera.

A tungsten wire (Nilaco, diameter: 50 μm) was used as a test sample, in order to estimate the spatial resolution of the lens-coupling detector system. The nine projection images were successfully acquired at the same time with a frame rate of 2000 fps, as shown in Fig. 2. The beam numbers L1–L4 and R1–R4 are defined in Fig. 1, and the projection angles are shown in Fig. 2. The corresponding X-ray energies for the Si 220 Bragg reflection are 20.6 keV, 24.9 keV, 32.2 keV, and 46.5 keV for the L1 and R1, L2 and R2, L3 and R3, and L4 and R4 beams, respectively. The contrast of the images obtained by the L3, L4, R3, and R4 beams are lower as compared to the other images with lower X-ray energies, since the transmittance increases with X-ray energy. The FWHM of the profile across the wire width, averaged for the images obtained by the L1, L2, R1, and R2 beams, was 120 ± 7 μm, indicating that the spatial resolution of the detector was about 70 μm which was mainly determined by the thickness of the scintillator screens (50 μm) and the pixel size of the CMOS camera (20 μm). The spatial resolution is much better than that of the detector system with the branched optical fiber bundle, about 200 μm.[46] The resolution of the fiber-coupling system would be largely restricted by the surface roughness of the optical fibers.

To demonstrate the capability for the time-resolved imaging, we observed the moment of breaking of a light-bulb filament (STANLEY MA302, 14 V/60 mA) caused by an overload (100 V, 0.24 A). Fig. 3 shows the projection images (natural logarithm of the X-ray transmittance) made by the white SR, L1, L2, R1, and R2 beams, captured (a) before, (b) during, and (c) after the breaking. Each image was captured successively at a frame rate of 2000 fps. The movies for the nine projection images are provided in the Supplementary data. Note that we surrounded the light bulb with a black-painted polyimide tape to reduce the background light emitted from the glowing light bulb; the small dots seen in the images made by the white SR beam originated from air bubbles formed in between the polyimide tape and light bulb.

In the beginning of the breaking, the left half of the filament was deformed as seen in Fig. 3(b): the bending points A and B indicated by the arrows were clearly observed. Three ms later, the right half of the filament began to deform (see the Supplementary data), and eventually the filament was completely broken at point C as clearly seen in Fig. 3(c). We estimated the amount of displacement of point D indicated in Fig. 3(c) from its original position in Fig. 3(a). By linear least-squares fitting to the change of pixel position in the images obtained by the white SR, L1, R1, and R2 beams, the amount of displacement along the depth direction, here defined as the direction of the L2 beam, was estimated to be -0.12 mm.

We also show a movie of a ladybug in the other Supplementary data. A motion of its leg was successfully captured by the white SR, L1, L2, R1, and R2 beams at a frame rate of 2000 fps, suggesting the possible capability of *in-vivo* observation of living beings.

In summary, we performed a high-speed multi-beam X-ray imaging by using a detector system and the multi-beam X-ray optics.[45] We utilized optical relay lenses and mirrors for connecting four scintillator screens to a CMOS camera, and successfully obtained nine projection images of a sample at once with an exposure time of 0.5 ms, without moving the sample, X-ray source, and detector. The spatial resolution estimated from a tungsten wire (50 µm diameter) test sample was 70 µm, which is better than that of the previously reported optical fiber-coupling detector, 200 µm.[46)] The moment of breaking of a light-bulb filament and a motion of a ladybug were successfully captured with a temporal resolution of 0.5 ms, demonstrating the capability for the high-speed and high-spatial-resolution multi-beam X-ray imaging. The detector system can be potentially extended to capture all the ~30 beams, distributed in an angular range of about ±70˚, to realize the high-speed 4D tomography.

Acknowledgments

This research was supported by JST CREST Grant No. JPMJCR 1765. The experiment was performed in SPring-8, Japan (Proposal No. 2019B1074). The holder of the multi-beam X-ray optics was fabricated in the machine shop of IMRAM, Tohoku University.

References

1) A. Snigirev, I. Snigireva, V. Kohn, S. Kuznetsov, and I. Schelokov, Rev. Sci. Instrum. **66**, 5486 (1995).

2) S. W. Wilkins, T. E. Gureyev, D. Gao, A. Pogany, and A. W. Stevenson, Nature **384**, 335 (1996).

3) P. Cloetens, R. Barrett, J. Baruchel, J.-P. Guigay, and M. Schlenker, J. Phys. D: Appl. Phys. **29**, 133 (1996).

4) C. David, B. Nöhammer, and H. H. Solak, Appl. Phys. Lett. 81, 3287 (2002).

5) A. Momose, S. Kawamoto, I. Koyama, Y. Hamaishi, K. Takai, and Y. Suzuki, Jpn. J. Appl. Phys. **42**, L866 (2003).

6) T. Weitkamp, A. Diaz, C. David, F. Pfeiffer, M. Stampanoni, P. Cloetens, and E. Ziegler, Opt. Express **13**, 6296 (2005).

7) A. Momose, W. Yashiro, and Y. Takeda, Jpn. J. Appl. Phys. **45**, 5254 (2006).

8) F. Pfeiffer, T. Weitkamp, O. Bunk, and C. David, Nat. Phys. **2**, 258 (2006).

9) W. Yashiro, Y. Takeda, and A. Momose, J. Opt. Soc. Am. A **25**, 2025 (2008).

10) A. Momose, W. Yashiro, and Y. Takeda, Jpn. J. Appl. Phys. **47**, 8077 (2008).

11) F. Pfeiffer, T. Weitkamp, O. Bunk, and C. David, Nat. Mater. **7**, 134 (2008).

12) W. Yashiro, Y. Takeda, A. Takeuchi, Y. Suzuki, and A. Momose, Phys. Rev. Lett. **103**,

180801 (2009).

13) A. Momose, W. Yashiro, H. Maikusa, and Y. Takeda, Opt. Express **17**, 12540 (2009).

14) W. Yashiro, Y. Terui, K. Kawabata, and A. Momose, Opt. Express **18**, 16890 (2010).

15) W. Yashiro, S. Harasse, A. Takeuchi, Y. Suzuki, and A. Momose, Phys. Rev. A **82**, 043822 (2010).

16) H. Kuwabara, W. Yashiro, S. Harasse, H. Mizutani, and A. Momose, Appl. Phys. Express **4**, 062502 (2011).

17) A. Momose, H. Kuwabara, and W. Yashiro, Appl. Phys. Express **4**, 066603 (2011).

18) W. Yashiro, S. Harasse, K. Kawabata, H. Kuwabara, T. Yamazaki, and A. Momose, Phys. Rev. B **84**, 094106 (2011).

19) W. Yashiro and A. Momose, Opt. Express **23**, 9233 (2015).

20) W. Yashiro, P. Vagovič, and A. Momose, Opt. Express **23**, 23462 (2015).

21) W. Yashiro, C. Kamezawa, D. Noda, and K. Kajiwara, Appl. Phys. Express **11**, 122501 (2018).

22) W. Yashiro, D. Noda, and K. Kajiwara, Opt. Express **26**, 1012 (2018).

23) W. Yashiro, Microscopy **67**, 303 (2018).

24) W. Yashiro, S. Ikeda, Y. Wada, K. Totsu, Y. Suzuki, and A. Takeuchi, Sci. Rep. **9**, 14120 (2019).

25) J. J. Socha, M. W. Westneat, J. F. Harrison, J. S. Waters, and W. K. Lee, BMC Biol. **5**, 6 (2007).

26) J. S. Lee, B. M. Weon, S. J. Park, J. H. Je, K. Fezzaa, and W. K. Lee, Nat. Commun. **2**, 367 (2011).

27) A. Rack, M. Scheel, L. Hardy, C. Curfs, A. Bonnin, and H. Reichert, J. Synchrotron Rad. **21**, 815 (2014).

28) W. Yashiro, D. Noda, and K. Kajiwara, Appl. Phys. Express **10**, 052501 (2017).

29) W. Yashiro, R. Ueda, K. Kajiwara, D. Noda, and H. Kudo, Jpn. J. Appl. Phys. **56**, 112503 (2017).

30) M. P. Olbinado et al., Opt. Express **25**, 13857 (2017).

31) M. P. Olbinado, J. Grenzer, P. Pradel, T. De Resseguier, P. Vagovic, M.-C. Zdora, V. A. Guzenko, C. David, and A. Rack, J. Instrum. **13**, C04004 (2018).

32) E. M. Escauriza, M. P. Olbinado, M. E. Rutherford, D. J. Chapman, J. C. Z. Jonsson, A. Rack, and D. E. Eakins, Appl. Opt. **57**, 5004 (2018).

33) P. Vagovič et al., Optica **6**, 1106 (2019).

34) F. García-Moreno, P. H. Kamm, T. R. Neu, F. Bülk, R. Mokso, C. M. Schlepütz, M.

Stampanoni, and J. Banhart, Nat. Commun. **10**, 3762 (2019).

35) A. Momose, W. Yashiro, H. Maikusa, and Y. Takeda, Opt. Express **17**, 12540 (2009).

36) A. Momose, W. Yashiro, S. Harasse, and H. Kuwabara, Opt. Express **19**, 8423 (2011).

37) D. P. Finegan, M. Scheel, J. B. Robinson, B. Tjaden, I. Hunt, T. J. Mason, J. Millichamp, M. Di Michiel, G. J. Offer, G. Hinds, D. J. L. Brett, and P. R. Shearing, Nat. Commun. **6**, 6924 (2015).

38) A. Ruhlandt, M. Töpperwien, M. Krenkel, R. Mokso, and T. Salditt, Sci. Rep. **7**, 6487 (2017).

39) M. H. Li, H. Q. Yang, and H. Kudo, Phys. Med. Biol. **47**, 2599 (2002).

40) D. L. Donoho, IEEE Trans. Inf. Theory **52**, 1289 (2006).

41) Y. Ye, H. Yu, Y. Wei, and G. Wang, Int. J. Biomed. Imaging **2007**, 63634 (2007).

42) H. Kudo, M. Courdurier, F. Noo, and M. Defrise, Phys. Med. Biol. **53**, 2207 (2008).

43) M. Hoshino, T. Sera, K. Uesugi, and N. Yagi, J. Instrum. **8**, C05002 (2013).

44) P. Villanueva-Perez et al., Optica **5**, 1521 (2018).

45) W. Voegeli, K. Kajiwara, H. Kudo, and W. Yashiro Optica **7**, 514 (2020).

46) W. Yashiro, T. Shirasawa, C. Kamezawa, W. Voegeli, E. Arakawa, and K. Kajiwara, Jpn. J. Appl. Phys. **59**, 038003 (2020).

Figure Captions

Fig. 1. Schematic illustration of the experimental layout of the multi-beam X-ray imaging using the lens-coupling detector system. Inset at the bottom: photo of the detector system.

Fig. 2. Projection images (X-ray transmittance) of the tungsten wire, simultaneously recorded by the multi-beam X-ray imaging detector with an exposure time of 0.5 ms [gray scale: 0–1.2]. The projection angles are shown in the parentheses.

Fig. 3. Projection images (natural logarithm of X-ray transmittance) of the light bulb, simultaneously recorded by the multi-beam X-ray imaging detector at a frame rate of 2000 fps [gray scale: -1.5–0.2 for the white SR beam and -2.5–0.2 for the other beams]. (a) The images recorded before the filament was broken (corresponding to the images at 4 ms of the supplementary movie). (b) and (c) The images recorded 2 ms and 7 ms later from (a), respectively.

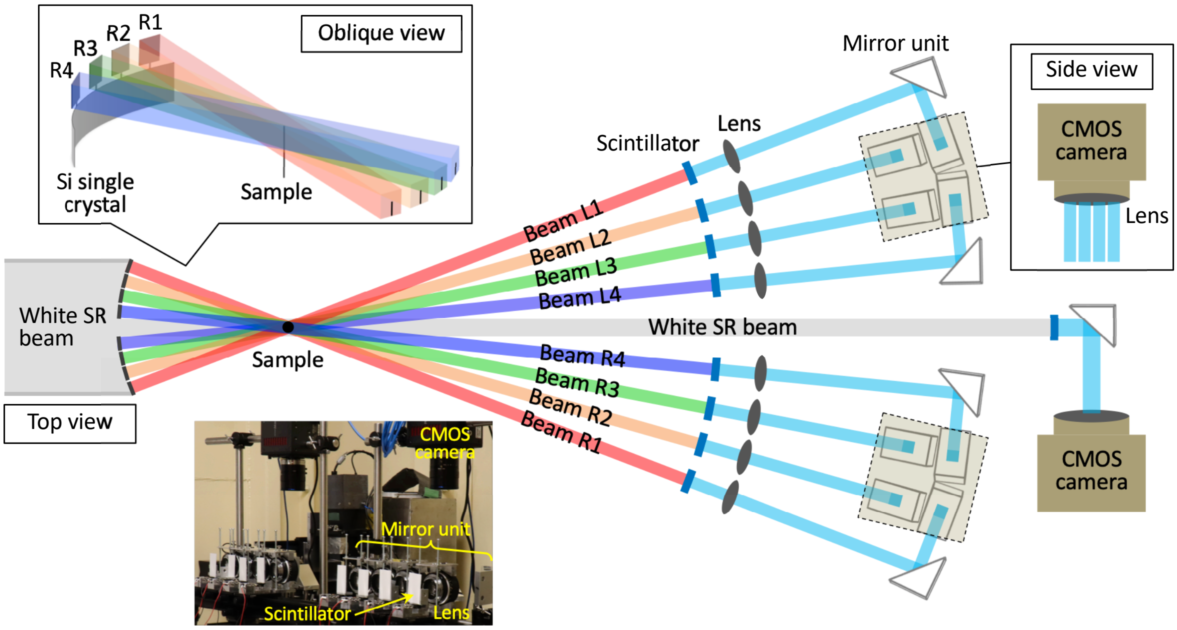

Fig.1. Schematic illustration of the experimental layout of the multi-beam X-ray imaging using the lens-coupling detector system. Inset at the bottom: photo of the detector system.

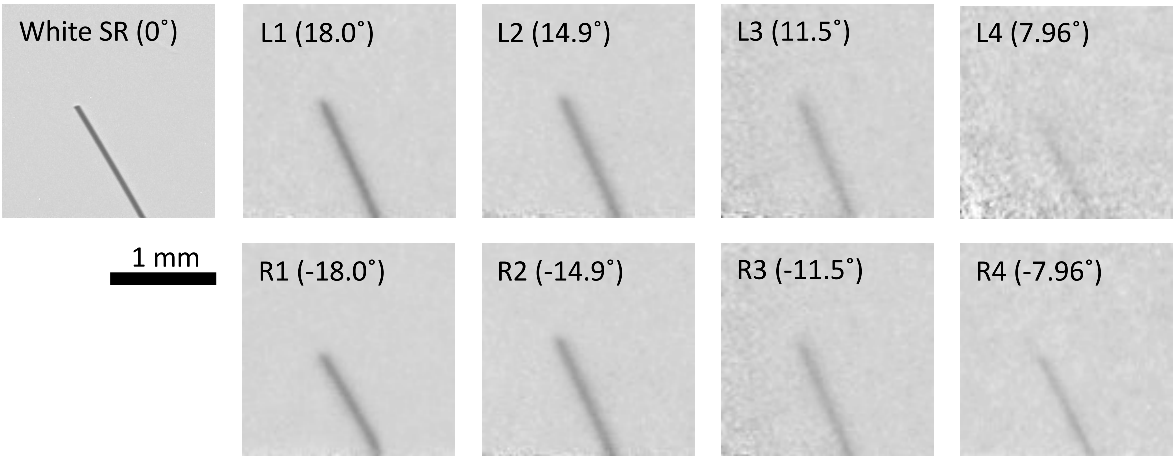

Fig. 2. Projection images (X-ray transmittance) of the tungsten wire, simultaneously recorded by the multi-beam X-ray imaging detector with an exposure time of 0.5 ms [gray scale: 0–1.2]. The projection angles are shown in the parentheses.

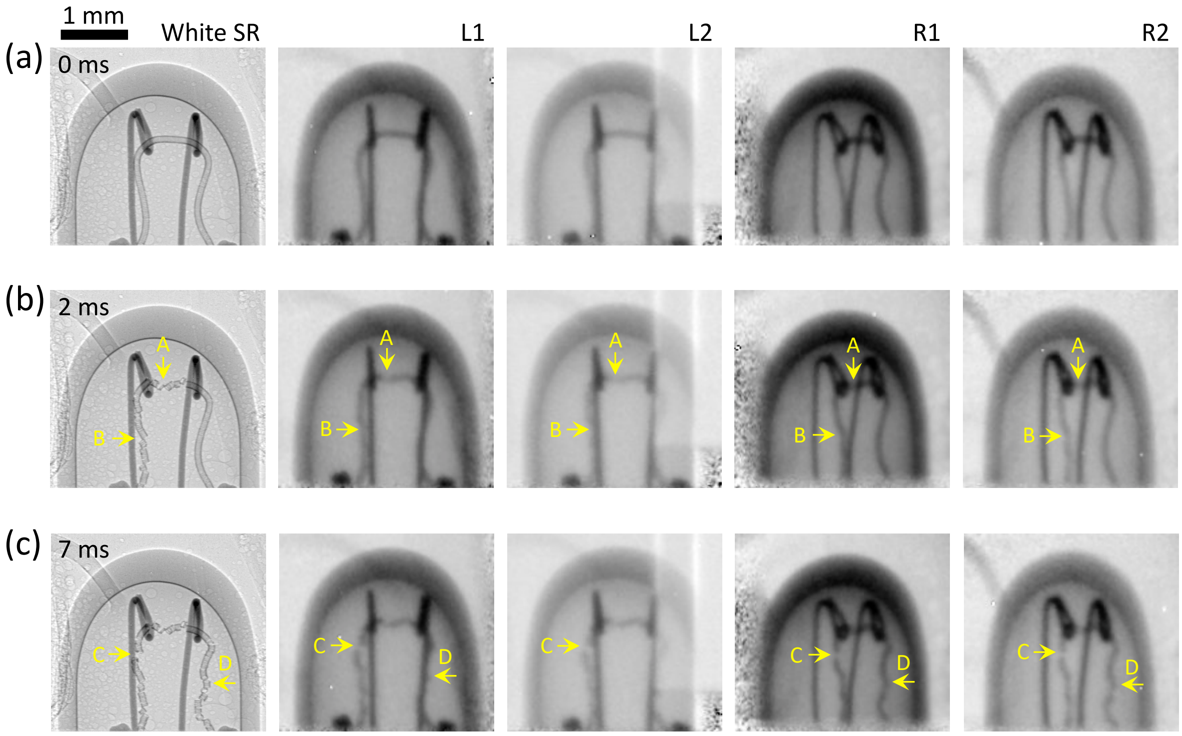

Fig. 3. Projection images (natural logarithm of X-ray transmittance) of the light bulb, simultaneously recorded by the multi-beam X-ray imaging detector at a frame rate of 2000 fps [gray scale: -1.5–0.2 for the white SR beam and -2.5–0.2 for the other beams]. (a) The images recorded before the filament was broken (corresponding to the images at 4 ms of the supplementary movie). (b) and (c) The images recorded 2 ms and 7 ms later from (a), respectively.